Full length article

Fractional Frequency Reuse in Ultra Dense Networks

Sinh Cong Lam [a],[*], Xuan Nam Tran [b]

[a] University of Engineering and Technology, Vietnam National University, Hanoi, Viet Nam
[b] Advanced Wireless Communications Group, Le Quy Don Technical University, Hanoi, Viet Nam

ARTICLE INFO

ABSTRACT

Ultra Dense Network (UDN) in which Base Stations (BSs) are deployed at an ultra high density is a promising network model of the future wireless generation. Due to ultra densification, reuse of frequency bands with an ultra high density is compulsory for this network. Conventionally, the research on frequency reuse technique such as Fractional Frequency Reuse (FFR) classifies the active users into only two groups. However, this approach is not suitable for UDNs where the signal experiences a huge amount of power loss over distances. Thus, this paper proposes a generalized model of FFR for UDNs where the active users are classified into more than two groups The paper introduces a simple approach to obtain the coverage probability of a typical user in the case of a general path loss model. In the case of stretched path loss model for UDNs, the closed-form expression of user coverage probability is derived. From the analytical and simulation results, it is stated that the proposed model can improve user performance without increasing BS power consumption. Furthermore, two additional interesting conclusions are found in this paper: *(i)* the user coverage probability increases to a peak before passing a decline when the density of BSs increases; *(ii)* an increase in BS transmission power may decrease the user performance.

1. Introduction

In recent years, the number of networked devices has risen critically. According to Cisco report [1], the number of networked devices in 2023 will reach 29.3 billion which are about 3 times greater than the world population. This will make the mobile data traffic increase by 8 times in the next few years. The explosive growth has encouraged the development of new generations of mobile networks, particularly 5G, to provide the ultra-high data rate, ultra-low latency, ultra-high number of connections as well as ultra-wide coverage area [2,3]. To meet the requirements of 5G networks, Ultra Dense Networks (UDNs) in which the distance between two adjacent Base Stations (BSs) is around 10 m has been introduced as a promising solution [4–6]. The millimeter wave (mmWave) is recognized as the ideal operational frequency bands for UDNs.

However, the deployment of BSs with an ultra-high density introduces new challenges. Specifically, the power loss of the transmitted signal should be carefully investigated since the mmWave is extremely sensitive to the transmission environment. Moreover, the interference between cells cannot be ignored when the BSs are very close together. Therefore, a large number of research works have been conducted to investigate UDN performance through path loss modeling and intercell interference coordination technique.

The performance of wireless systems strongly depends on the power loss of the radio signal. To analyze the network performance, the path loss model should be studied first. The multi-slope path loss model in which the signal experiences more than one path loss exponents was widely studied [7–10]. For each slope, the power loss follows the conventional model which is formulated as $Loss = r^{-\alpha}$, where r and α are the horizontal distance and the path loss exponent, respectively. The authors based on the probability of Line-of-Sight (LoS) and non-Line-of-Sight (nLoS) to compute the power loss over the wireless link. The coverage probability and spectrum efficiency were analyzed. The impacts of the density of BSs and their heights were examined [11–13]. Other related works modeled the power loss as a exponential function of the distance such as [14,15]. Recently, the Stretched Path Loss Model (SPLM) was introduced in Ref. [16]. In this model, the power loss over a distance of r is determined as αr^{β} in which α and β are turnable parameters. This model is considered a simplified model of a multi-slop model with a finite number of slopes. Through experimental measurements, the authors proved that the SPLM is more suitable for UDNs than previous models in the literature. Thus, we utilize this model to analyze the UDNs.

Frequency Reuse is a popular technique in wireless communications that allows two BSs to share their frequency bands.

The demand for reuse of frequencies became more necessary in the 4G networks since these systems require much more BSs to cover the service area than its previous generations. Thus, the Frequency Reuse technique has been improved to allow adjacent BSs to transmit on the same frequency bands at the same time. This technique is known as Fractional Frequency Reuse (FFR). FFR was originally used to define reuse of frequency between cells where each BS is allowed to utilize a part of whole frequency bands. For such definition, *FFR with reuse factor of N* means that every N adjacent BSs employ the same frequency reuse pattern and each BS is allocated $1/N$ of whole frequency bands. It is reminded that the term *frequency reuse pattern* is used to describe the approach that the sub-bands are used in a group of N adjacent BSs. This term is commonly used in the documents of European Telecommunications Standards Institute (ESTI) such as in Ref. [17]. This original FFR scheme could not optimize radio spectrum efficiency. Thus, new FFR schemes such as Soft FFR, Strict FFR, and distributed FFR [18,19] have been introduced to allow each BS to utilize whole frequency bands. Due to the new introduction of FFR, the concept of FFR with reuse factor N is explained as following aspects: *(i)* each BS is allowed to utilize full bandwidth; *(ii)* every N adjacent BSs use the same frequency reuse pattern. Conventionally, FFR scheme divides the associated users and allocated frequency resources into 2 groups respectively so that each group of users is served by a group of frequency resources. By this way, the Intercell Interference (ICI) can be minimized and the user performance can be improved.

Although FFR has been well-investigated for 4G systems, the deployment of this technique for future cellular network systems is being at the early stage [20–25]. The authors in [20, 26] discussed the challenges and approaches of FFR utilization in the these systems. The effects of FFR algorithm on network performance were discussed in [23]. In that work, the optimal frequency reuse factor was derived to optimize energy and spectral efficiency. The authors in [25] introduced an approach to achieve load-balancing between macro and small BSs. Although these works derived important concepts about FFR techniques for future mobile systems, the classification of users into groups has not been well-discussed. The authors in [24] discussed the user classification. However, this work only performed simulation with the mmWave at 26-GHz band. Moreover, in all works discussed above, the two-phase operation of FFR algorithm has not been studied. This motivates us to model and examine the performance of FFR algorithm in UDNs.

The performance analysis of FFR for regular cellular networks with low densities of BSs has been conducted in some interesting works. Ref. [27] introduced an analytical approach and important initial results regarding to the effects of FFR on the cellular networks. In our recent work [28], the uplink performance with power control was considered. The closed-form expressions of performance metrics were given by utilizing Gaussian Quadrature. Recently, the author in [29,30] presented fully closed-form expression. However, these works only studied regular path loss models in which the received power over a distance of r is $Pr^{-\alpha}$ (P is the transmission power). In the case of UDNs, as discussed in the previous paragraphs, this path loss model is no longer suitable and should be replaced by SPLM. With the deployment of SPLM, the kernel integral of user performance metric expressions became more complicated [16,31]. Thus, the approaches in [28–30] are no longer applicable and the closed-form expressions were only found in the form of Polylogarithm function when $2/\beta$ is an integer number. This paper bases on the Taylor expansions to obtain the simple form of the performance metrics before utilizing confluent hypergeometric function and Gauss–Laguerre quadrature to derive their closed-form expressions for all cases of β. In the case of $2/\beta$, the closed-form expressions become more

simple forms which do not rely on confluent hypergeometric function.

Moreover, the works in the literature only discussed FFR with two user groups and two power levels which is equivalent to FFR with the reuse factor of 3. In our recent works [32], a general FFR algorithm with N user groups was introduced for sparse cellular networks with a low density of BSs and the regular path loss model. Conventionally, sparse cellular networks such as 3G, 4G work with a frequency range from 700 MHz - 4 GHz [33] while UDNs are recommended to work with mmWave radio signals whose frequencies are greater than 24 GHz [34]. Thus, the downlink signal and consequently SINR in sparse networks do not experience so fast attenuation as others in UDNs. Thus, an increase in the number of user groups N did not bring any benefit to the user performance as shown in [32]. In contrast, this paper indicates that the user coverage probability in UDNs is significantly improved when the number of user groups increases from 2 to 3 while the total power consumption remains unchanged.

Generally, compared to the aforementioned works in the literature, the contributions of this work are summarized as follows:

- We propose a generalized model of FFR for UDNs in which the users are classified into more than two groups. The analytical results show the proposed model can improve the user performance without increasing BS's power consumption.
- We introduce an approach to obtain the simple form of user coverage probability expression under a general path loss model. In the case of a regular path loss model, the user coverage probability is derived as a sum of elementary functions as in Corollary 3.3. In the case of SPLM, the closed-form expression is obtained by following confluent hypergeometric functions and Gauss quadratures as in Section 4.
- The analytical results that are verified by Monte Carlo simulation indicate that an increase in the density of BSs λ only improves the user coverage probability if λ is in a small regime such as $\lambda < 60$ BS/km^2 and $SNR = 20$ dB. In addition, higher transmission powers may result in a decline in the user coverage probability if both SNR and λ are in high regimes such as $SNR > 10$ dB and $\lambda = 180$ BS/km^2. Thus, if an increase in the density of BSs is compulsory for UDNs utilizing FFR, then reducing their transmission power is an effective solution.

2. System model

This paper studies single-tier UDNs in which BSs are distributed according to a spatial Poison Point Process (PPP) with mean λ (BS/km^2). The network is assumed to cover an infinite area. Thus, the number of BSs reaches infinity where all BSs are allowed to utilize the whole frequency bands. The distance from the typical user to other BSs may vary from 0 to ∞. Consequently, to analyze the performance of the typical user, the integrals of distances should be taken to ∞. In practical networks, only the BSs that are close enough to the typical user can have impacts on the performance of this user. Thus, the Monte Carlo simulation assumes that the networks cover a finite area of S where S needs to be large enough to cover all BSs that have impacts on the typical user.

It is supposed that all the signals traveling within the network area experiencing the same path loss model and Rayleigh fading with PDF $f(\gamma) = \exp(-\gamma)$. Denote L_r as the power loss over a distance of r. Thus, L_r is a decreasing function.

The user usually prefers a connection to BS n with the strongest average received signal strength. For example, the user associates with a BS at a distance of r if its average received

signal strength $PL_r > PL(r_k) \ \forall k \in \theta \setminus n$ or $r < r_k, \forall k \in \theta \setminus n$ where θ is the set of BSs in the networks. Thus, it is stated that in the case of the same path loss model, the BS with the highest average received signal of a user is the nearest BS of that user, .i.e the nearest association procedure. The PDF and CDF of r are respectively given by

$$f(r) = 2\pi\lambda \exp(-\pi\lambda r^2) \tag{1}$$

and $F(r) = 1 - \exp(-\pi\lambda r^2)$ (2)

The following table lists the all important notations in this paper

Notation	Description
λ	Density of BSs
N	Number of user groups
I_0	Interfering power of a user during establishment phase
I	Interfering power of a user during communication phase
$SINR^{(o)}$	SINR of a typical user during the establishment phase
$SINR_n$	SINR of a user in Group n during the communication phase
P_n	Serving power of users in Group n
$T_0, T_1, \dots, T_N$	SINR thresholds
$P_0, P_1, \dots, P_N$	Transmission powers
$\mathcal{P}_{An}$	Probability that a user is assigned to Group n
$\mathcal{P}_n$	Coverage probability of a typical user
$_1F_1(.,.,.)$	Confluent hypergeometric function of the first kind
$U(.,.,.)$	Confluent hypergeometric function of the second kind
$\Gamma(x,y)$	Incomplete Gamma function
σ^2	power of Gaussian noise

The operation of FFR can be modeled as two consecutive phases, .e.g. the establishment phase and communication phase. While the establishment phase has responsibility for user classification, the data exchange process is taken play during the communication phase. In the next section, we will discuss these phases in detail and derive the SINR expression for each phase.

2.1. Establishment phase

According to 3GPP specification [35], the received signal quality on the downlink control channel can be used for user classification purpose during the establishment phase. The establishment phase cycle can be adjustable and depends on characteristic of wireless environment. In particular networks, this phase can be taken place as soon as the user reports Channel Quality Indicator (CQI) which maybe every 40 ms.

In this work, we assume that UEs are classified into N groups by $N+1$ SINR thresholds, denoted by $T_0, T_2, \dots, T_N$ ($T_0 \leq T_2 \leq \cdots \leq T_N$). While T_0 and T_N are lower and upper bounds of SINR respectively, other values of $T_1, T_2, \dots, T_{N-1}$ can be chosen appropriately for specific purposes such as user performance optimization or minimize power consumption. The event that a user with downlink SINR on the control channel, $SINR^{(o)}(r)$, is assigned into Group n is defined as:

$$T_{n-1} < SINR^{(o)}(r) < T_n \tag{3}$$

In other words, it can be said that a group of users consists users that have the same SINR range. The corresponding probability is given by

$$\mathcal{P}_{An}(r) = \mathbb{P}\left[T_{n-1} < SINR^{(o)}(r) < T_n\right] \tag{4}$$

Because of utilizing the same transmission power P_N and sharing frequency resource between BSs, each control channel is affected by ICI from all adjacent BSs. Thus, total ICI power of a user on a downlink control channel during the establishment phase is given by:

$$I_o = \sum_{j \in \theta} P_N g_j^{(o)} L_{r_j} \tag{5}$$

where $g_j^{(o)}$ is the power gain of the channel from the user to interfering BS j, PDF of $g_j^{(o)}$ is $f(g_j^{(o)}) = \exp(-g_j^{(o)})$, and L_{r_j} is the power loss on the wireless link from user to its serving BS, $L_{r_j} = \exp(-\alpha r_j^\beta)$.

Thus, the SINR is obtained by:

$$SINR^{(o)}(r) = \frac{P_N g^{(o)} L_r}{I_o + \sigma^2} \tag{6}$$

where σ^2 is power of Gaussian noise.

Substituting Eq. (6) into Eq. (4), we obtain

$$\begin{aligned}
\mathcal{P}_{An}(r) &= \mathbb{P}\left[T_{n-1} < \frac{P_N g^{(o)} L_r}{I_o + \sigma^2} < T_n \,\middle|\, r\right] \\
&= \mathbb{P}\left[T_{n-1}\frac{I_o + \sigma^2}{P_N L_r} < g^{(o)} < T_n \frac{I_o + \sigma^2}{P_N L_r} \,\middle|\, r\right]
\end{aligned} \tag{7}$$

The probability above can be obtained from Appendix A with $\hat{T} = 0$. Hence, the association probability $\mathcal{P}_{An}(r)$ is given by

$$\mathcal{P}_{An}(r) = s_{n-1}\exp\left(-\frac{2\pi\lambda}{T_{n-1}}\upsilon(T_{n-1})\right) - s_n \exp\left(-\frac{2\pi\lambda}{T_n}\upsilon(T_n)\right) \tag{8}$$

in which

$$\upsilon(x)$$

$$= \begin{cases}
\left(\begin{aligned}
&\sum_{m=1}^{M}(-1)^{m-1}L_r^{m-1}x^{2-m}\int_r^{L_r^{-\frac{1}{x}}} r_j L_{r_j}^{1-m}dr_j \\
&+ \sum_{m=0}^{M}(-1)^m x^{m+2}L_r^{-1-m}\int_{L_r^{-\frac{1}{x}}}^{\infty} r_j L_{r_j}^{m+1}dr_j
\end{aligned}\right) & \text{for} \quad x > 1 \\[1em]
\sum_{m=0}^{M}(-1)^m x^{m+2}L_r^{-1-m}\int_r^\infty L_{r_j}^{m+1}r_j dr_j & \text{for} \quad x \leq 1
\end{cases} \tag{9}$$

and M is an integer and is selected so that the Taylor series in Eq. (A.6) converges. For sufficient computation, $M = 10$ is selected in this paper; $\hat{s} = \exp\left(-\frac{1}{L(r)}\frac{\hat{T}}{\gamma_N}\right)$ and $s_n = \exp\left(-\frac{1}{L(r)}\frac{T_n}{\gamma_N}\right)$.

The association probability of the typical user with Group n is obtained by

$$\begin{aligned}
\mathcal{P}_{An} = 2\pi\lambda \int_0^\infty \Bigg[&s_{n-1}\exp\left(-\frac{2\pi\lambda}{T_{n-1}}\upsilon(T_{n-1})\right) \\
&- s_n \exp\left(-\frac{2\pi\lambda}{T_n}\upsilon(T_n)\right)\Bigg] f(r)dr
\end{aligned} \tag{10}$$

where $f(r)$ is defined in Eq. (1).

2.2. Communication phase

With the deployment of FFR, all BSs are allocated the whole frequency bands. To serve N groups of users that are determined in the establishment phase, each BS also divides the allocated frequency bands into N orthogonal groups of sub-bands by which every N adjacent BSs utilize the same frequency reuse pattern. Conventionally, the ratio between the number of users from different groups is proportional to the number of allocated sub-bands. Fig. 1 gives an example of frequency reuse pattern with $N = 4$. As seen from this figure, a group of sub-bands (Group of Frequency, GF) that is used to serve a Group of Users (GU) will be re-used to serve a different group of users in adjacent
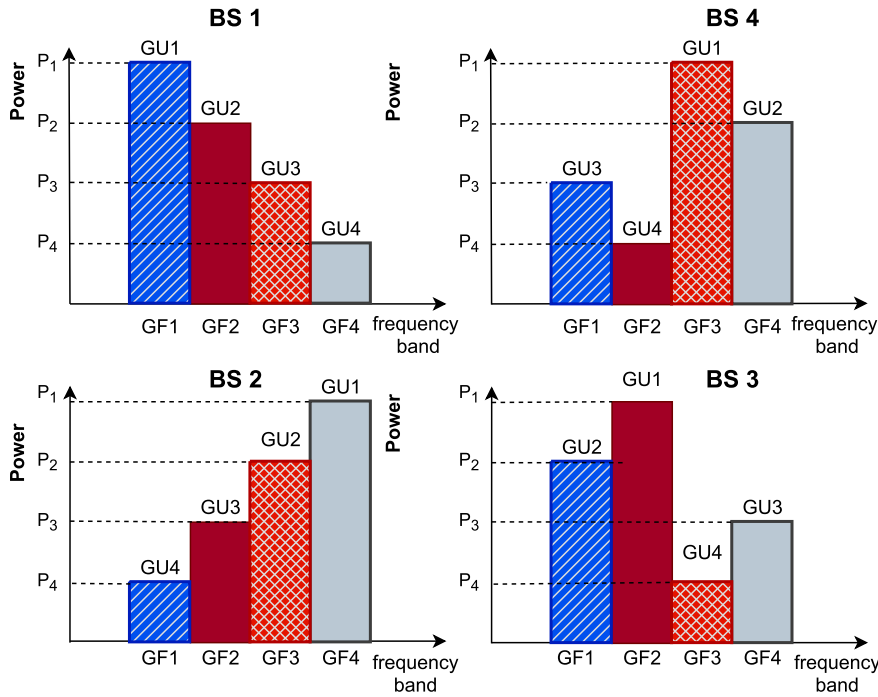
Fig. 1. An example of proposed FFR with $N = 4$. *GU: Group of UEs, GF: Group of Frequencies.*

cells. Take GF1 for example, GF1 is used to serve GU1 by BS1 but it is re-used to serve GU4 by BS2, GU3 by BS4. As in 3GPP specification [36], BSs are interconnected together by employing X2 interface with a latency of up to 10 ms. Conventionally, the scheduling mechanism re-allocates frequency resources for users every time slot, i.e. 1 ms. Thus, X2 interface is not possible to carry real-time resource allocation strategies between BSs. As a result, BSs can allocate the same sub-bands to their active users. Thus, when the number of users is large enough, all BSs may transmit on the same sub-bands at the same time. In addition, the groups of frequencies should not be changed to avoid bandwidth fragmentation, signaling overload, as well as ICI. Hence, this paper assumes that the groups of sub-bands are fixed during the communication phase.

While the establishment phase utilizes SINR on the control channel, data transmission process during the communication phase only depends on the data channel. In addition, the transmission power on control channels are the same for all BSs while the power levels on data channels are adjustable [35]. Thus, we assume that each group of users is served by a specific power level during the communication phase. In other words, each BS utilizes N power levels such as $P_1, P_2, \ldots, P_N$ ($P_1 \geq P_2 \geq \cdots \geq P_N$) in which Group n containing users with $T_{n-1} < SINR < T_n$ served by transmission power level P_n.

The lowest power level P_N is the transmission power on the control channel that can be used by a BS to communicate with nearby users. According to 3GPP specification [35], the transmission power of each BS should not dynamically change. Thus, each BS should select appropriate transmission power levels on each frequency group to optimize its operation. One of the main contributions of this paper is to analyze the effects of transmission power on user coverage probability.

Fig. 1 illustrates the communication phase of our proposed FFR model with $N = 4$ where every 4 adjacent BSs indexed by BS 1, BS 2, BS 3, and BS 4 forming a group of BSs. When only two power levels are applied, the proposed model becomes the well-known FFR schemes in the literature. For example,

- $P_3 = P_4 = 0$, the proposed model degrades into Strict FFR [18].
- $P_2 = P_3 = P_4$ the proposed model corresponds to Soft FFR [19]

In a given group, a user in Group 1 (GU1) of BS 1 can be affected by ICI from adjacent BSs transmitting on Group of Frequencies 1 (GF1), particularly BSs 2, 3, and 4 with corresponding transmission power are P_4, P_3 and P_2. Since the frequency reuse pattern is repeated in every group of 4 adjacent BSs, this user is also affected by interference from BS 1 on GF 1 in other BSs' groups.

In general, the interfering BSs can be classified into N groups where interfering group k transmits at a power level of P_k during the communication phase. Let λ_k as the density of interfering BSs in Group k. Then $\bigcup_{k=1}^{N} \theta_k = \theta$ and $\sum_{k=1}^{N} \lambda_k = \lambda$. The ICI power of a typical user from BSs in Group k is determined by

$$I_k = P_k \sum_{j \in \theta_k} g_j L_{r_j} \tag{11}$$

where r_j and g_j are the distance and channel power gain from the typical user to its interfering BS j in Group k.

The total ICI power at the typical user is given by

$$I = \sum_{k=1}^{N} P_k \sum_{j \in \theta_k} g_j L_{r_j} \tag{12}$$

The downlink SINR of a user in Group n during the communication phase is

$$SINR_n(r) = \frac{P_n g L_r}{\sum_{k=1}^{N} P_k \sum_{j \in \theta_k} g_j L_{r_j} + \sigma^2} \tag{13}$$

where g and r are channel power gain and distance from the user to its serving BS respectively.

It is seen from Eq. (13) that BS j is considered to have a negative effect on $SINR_n(r)$ if L_{r_j} is large enough, i.e. r_j is small enough. Moreover, $r_j > r$ due to the assumption of the nearest association procedure. Therefore, BS j is considered the interfering source of

the user if the value of r_j is around that of r, i.e. $r_j \gtrsim r$. This condition will be utilized to derive the closed-form expression of the user coverage probability.

3. Performance evaluation

3.1. Definition metrics

Coverage probability of a user in group n. The user in Group n is under network coverage if

(1) Its downlink SINR during the establishment phase satisfies Inequality (3)
(2) Then, its downlink SINR during the communication phase is greater than the pre-defined coverage threshold $\hat{T}$

Therefore, the coverage probability of the user in Group n is formulated as the following conditional probability

$$\mathcal{P}_n(\hat{T}) = \mathbb{P}\left(SINR_n(r) > \hat{T} | T_{n-1} < SINR^{(o)}(r) < T_n\right) \quad (14)$$

in which

- $T_{n-1} < SINR^{(o)}(r) < T_n$ is the event that the user associates with Group n
- $SINR_n(r) > \hat{T}$ is to ensure that the received SINR of the user during the communication phase is greater than the required SINR for successful data transmission.

The coverage probability definition in Eq. (14) covers other definitions in related works in the literature such as:

- The definition in Refs. [18,37] for single group of users can be obtained by selecting $N = 1$, $T_0 = 0$ and $T_1 = \infty$.
- The definition in Refs. [27,38] for two groups of users corresponds to $N = 2$, $T_1 = 0$, $T_1 = T$ and $T_2 = \infty$.

For particular cellular systems, in order to obtain ultimate user experience for high speed data services such as video streaming and gaming, the minimum required SINR is $SINR(dB) \approx -5$ dB [39].

Theorem 3.1. *The coverage probability of the user in Group n is given by*

$$\mathcal{P}_n = \frac{2\pi\lambda}{\mathcal{P}_{An}} \int_0^\infty \hat{s}$$
$$\times \left[\begin{pmatrix} s_{n-1} \prod_{k=1}^N \exp\left[\frac{-2\pi\lambda_k}{\hat{T}\frac{\gamma_k}{\gamma_n} - T_{n-1}}\left(\upsilon\left(\hat{T}\frac{\gamma_k}{\gamma_n}\right) - \upsilon(T_{n-1})\right)\right] \\ -s_n \prod_{k=1}^N \exp\left[\frac{-2\pi\lambda_k}{\hat{T}\frac{\gamma_k}{\gamma_n} - T_n}\left(\upsilon\left(\hat{T}\frac{\gamma_k}{\gamma_n}\right) - \upsilon(T_n)\right)\right] \end{pmatrix} \right]$$
$$\times f(r)dr$$
$$(15)$$

Proof. See Appendix A. □

Coverage probability of a typical user. The typical user is located at a random position in the network and can be assigned to any group. Thus, the coverage probability of the typical user is defined as

$$\mathcal{P}(\hat{T}) = \sum_{n=1}^N \mathbb{E}\left[\mathcal{P}_n(\hat{T}|r)\mathcal{P}_{An}(r)\right] \quad (16)$$

in which

- $\mathcal{P}_n(\hat{T}|r)$ is the coverage probability of the user at distance r from its serving BS.

- $\mathcal{P}_{An}(r)$ is the probability of that user to be assigned into Group n

Taking the expected value with respect to variable r, we get

$$\mathcal{P}(\hat{T}) = 2\pi \sum_{n=1}^N \lambda_n \int_0^\infty \mathbb{E}\left[\mathcal{P}_n(\hat{T}|r)\mathcal{P}_{An}(r)\right] \exp\left(-\pi\lambda r^2\right) r dr \quad (17)$$

Corollary 3.2. *The coverage probability of the typical user is given by*

$$\mathcal{P}(\hat{T}) = 2\pi \sum_{n=1}^N \lambda_n$$
$$\times \int_0^\infty \left[\begin{pmatrix} \prod_{k=1}^N \hat{s}s_{n-1} \exp\left[-\frac{2\pi\lambda_k}{\hat{T}\frac{\gamma_k}{\gamma_n} - T_{n-1}}\left(\upsilon\left(\hat{T}\frac{\gamma_k}{\gamma_n}\right) - \upsilon(T_{n-1})\right)\right] \\ -\prod_{k=1}^N \hat{s}s_n \exp\left[-\frac{2\pi\lambda_k}{\hat{T}\frac{\gamma_k}{\gamma_n} - T_n}\left(\upsilon\left(\hat{T}\frac{\gamma_k}{\gamma_n}\right) - \upsilon(T_n)\right)\right] \end{pmatrix} \right]$$
$$\times \exp(-\pi\lambda r^2) r dr$$
$$(18)$$

Proof. The coverage probability in Eq. (16) is re-formulated as follows

$$\mathcal{P}(\hat{T}) = \sum_{k=1}^N \mathbb{E}\left[\mathbb{P}\left(SINR(r) > \hat{T} | T_{n-1} < SINR^{(o)}(r) < T_n\right) \right.$$
$$\left. \times \mathbb{P}\left(T_{n-1} < SINR^{(o)}(r) < T_n\right)\right]$$
$$= \sum_{k=1}^N \mathbb{E}\left[\mathbb{P}\left(SINR(r) > \hat{T}, T_{n-1} < SINR^{(o)}(r) < T_n\right)\right] \quad (19)$$

where (19) is obtained by following the Bayes rule.

Using the result of Appendix A, the desired result is given. □

The expressions of user coverage probability P_n in Eqs. (15) and (18) can cover all related cases in the literature. For example, the results in [27] refer to N = 2 and threshold $T_1 = 0$, $T_2 = T$ and $T_3 = \infty$. $\mathcal{P}_1$ and $\mathcal{P}_2$ corresponds to coverage probability of Cell-Center User and Cell-Edge User, respectively.

Furthermore, this expression is much more simple than related previous expressions in the literature for $N \leq 2$ such as [16,27]. Take the regular path loss model in which the path loss over a distance of r and the path loss exponent τ is $r^{-\tau}$ for example, the integral of $\upsilon(x)$ has a form of $\int_a^\infty y^{-z} dy$ $(z > 0)$ and can be computed easily.

Corollary 3.3. *For regular path loss model and $N = 1$, the closed-form expression of user coverage probability can be simply obtained in both cases of noise-limited networks and regular networks.*

Proof. Substituting $L_r = r^{-\alpha}$ into Eq. (9), we obtained

$$\upsilon(x)$$
$$= \begin{cases} r^2 \sum_{m=0}^M (-1)^m \left(\frac{x^{2/\alpha+1} - x^{1-m}}{\alpha m + 2} + \frac{x^{2/\alpha+1}}{\alpha m - 2}\right) & for \quad x > 1 \\ r^2 \sum_{m=0}^M (-1)^{m+1} x^{m+2} \frac{1}{2 - \alpha(m+1)} & for \quad x \leq 1 \end{cases}$$
$$(20)$$

Thus, $\upsilon(x)$ has a form of $\upsilon(x) = K(\hat{T})r^2$. The user coverage probability in Eq. (18) in the case of $N = 1$ has the form of

$$\mathcal{P}(\hat{T}) = \pi\lambda \int_0^\infty \exp\left(-\frac{\hat{T}}{\gamma}r^{\alpha/2} - \left(\frac{2\pi\lambda}{\hat{T}}K(\hat{T}) + \pi\lambda\right)r\right) dr \quad (21)$$

In regular networks, the closed-form expression $\mathcal{P}(\hat{T})$ can be obtained from Refs. [29,30] with parameters of $A = \frac{\hat{T}}{\gamma}$ and $B = \left(\frac{2\pi\lambda}{\hat{T}}K(\hat{T}) + \pi\lambda\right)$. Since parameter B in [29,30] is in the form of the infinity integral, the obtained closed-form expressions of our approach should be more simple.

In the noise-limited network, the closed-form expression is found as follows

$$\mathcal{P}(\hat{T}) = \frac{1}{\frac{2}{\hat{T}}K(\hat{T}) + 1} \tag{22}$$

Some works have derived the closed-form expressions in the case of noise-limited network such as [27,40]. In the normal networks, these expressions still have an infinity integral. The expression in Eq. (22) is exactly closed-form since it is represented through a limited number of standard operations. □

The power consumption. Since a user at a distance r from its serving BS is assigned to Group n and served by a power level of P_n with a probability of P_{An}, the power consumption of a BS, which is utilized to serve this user is

$$\overline{P}_n = P_n P_{An} \tag{23}$$

in which P_{An} is defined in Eq. (8).

The power consumption of the BS uses to serve the typical user is obtained by

$$\overline{P} = \sum_{n=1}^{N} \int_0^\infty P_n P_{An} f(r) dr \tag{24}$$

4. Approximated expressions for stretched path loss model

The path loss under SPLM over distance r is defined by $L_r = \exp(-\alpha r^\beta)$ where α and β are tunable parameters. The inverse function of SPLM is $L^{-1}(x) = \left(-\frac{\log x}{\alpha}\right)^{1/\beta}$.

It is seen from Eqs. (10), (15) and (18) that the performance metrics are the functions of $\upsilon(x)$. To find the closed-form of the performance metrics, the closed-form expression of $\upsilon(x)$ should be derived first.

Theorem 4.1. *The closed-form expression of $\upsilon(x)$ is given by*

$\upsilon(x)$
$$= \begin{cases} \frac{x}{2}\sum_{m=1}^{M}(-1)^{m-1}\left(\begin{matrix}\left(\frac{\tau_x}{\alpha}\right)^{2/\beta}{}_1F_1\left(1, 1+\frac{2}{\beta}, (1-m)\tau_x\right) \\ -r^2 x^{1-m}{}_1F_1\left(1, 1+\frac{2}{\beta}, (1-m)\tau_1\right)\end{matrix}\right) & \text{for } x > 1 \\ +\frac{x}{\beta}\sum_{m=1}^{M+1}(-1)^{m-1}(\alpha m)^{-2/\beta}U\left(1-\frac{2}{\beta}, 1-\frac{2}{\beta}, m\tau_x\right) \\ \frac{1}{\beta}\sum_{m=1}^{M+1}(-1)^{m-1}x^{m+1}(\alpha m)^{-2/\beta}U\left(1-\frac{2}{\beta}, 1-\frac{2}{\beta}, m\tau_1\right) & \text{for } x \leq 1 \end{cases} \tag{25}$$

in which

- $\tau_x = \alpha r^\beta + \log(x)$ *and* $\tau_1 = \alpha r^\beta$.
- ${}_1F_1(.,.,.)$ *is confluent hypergeometric function of the first kind*
- $U(.,.,.)$ *is confluent hypergeometric function of the second kind*

4.1. When $2/\beta$ is an integer

When $2/\beta$ is an integer, $\upsilon(x)$ can be obtained by

$\upsilon(x)$
$$= \begin{cases} \left(\begin{matrix}x\frac{\beta}{2}\frac{1}{(2/\beta)!}\sum_{\omega=1}^{2/\beta}\left(\begin{matrix}\frac{\tau_x^{2/\beta}}{\alpha^{2/\beta}}\tau_x^{-\omega} \\ -r^2\tau_1^{-\omega}\end{matrix}\right)\sum_{m=1}^{M}\frac{(-1)^{m-1}}{(1-m)^\omega} \\ +x\frac{(2/\beta-1)!}{\alpha^{2/\beta}}\sum_{\omega=1}^{2/\beta}\frac{\tau_x^{\omega-1}}{(\omega-1)!}\sum_{m=1}^{M+1}\frac{(-1)^{m-1}}{m^{2/\beta-\omega+1}}\end{matrix}\right) & \text{for } x > 1 \\ x\frac{(2/\beta-1)!}{\alpha^{2/\beta}}\sum_{\omega=1}^{2/\beta}\frac{\tau_1^\omega}{(\omega-1)!}\sum_{m=1}^{M+1}\frac{(-x)^m}{(m+1)^{2/\beta-\omega+1}} & \text{for } x \leq 1 \end{cases} \tag{26}$$

Proof. See Appendix B. □

Lemma 4.2. *The association probability of user in Group n in Eq. (10) and the coverage probability of the typical user in Eq. (16) can be expressed by the following approximated closed-forms*

$$\mathcal{P}_A = \sum_{m=1}^{M_G}\omega_j\left[\zeta\left(T_{n-1}, 0, r = \sqrt{\frac{t_i}{\pi\lambda}}\right) - \zeta\left(T_n, 0, r = \sqrt{\frac{t_i}{\pi\lambda}}\right)\right] \tag{27}$$

$$\mathcal{P}_n = \frac{\sum_{m=1}^{M_G}\omega_j\left[\zeta(T_{n-1}, \hat{T}, r) - \zeta(T_n, \hat{T}, r = \sqrt{\frac{t_i}{\pi\lambda_n}})\right]}{\sum_{m=1}^{M_G}\omega_j\left[\zeta(T_{n-1}, 0, r = \sqrt{\frac{t_i}{\pi\lambda_n}}) - \zeta(T_n, 0, r = \sqrt{\frac{t_i}{\pi\lambda_n}})\right]} \tag{28}$$

$$\mathcal{P}(\hat{T}) = \sum_{n=1}^{N}\sum_{m=1}^{N_G}\omega_j$$
$$\times\left[\zeta\left(T_{n-1}, \hat{T}, r = \sqrt{\frac{t_i}{\pi\lambda_n}}\right) - \zeta\left(T_n, \hat{T}, r = \sqrt{\frac{t_i}{\pi\lambda_n}}\right)\right] \tag{29}$$

where N_G is the degree of the Laguerre polynomial, t_i and w_i are the ith node and weight of the quadrature, respectively.

Proof. The desired results are obtained by using a change of variable $y = \pi\lambda r^2$, $y = \pi\lambda_n r^2$ and utilizing the Gauss–Laguerre [41] which states that $\int_0^\infty f(t)e^{-t} \approx \sum_{i=1}^{N_{GL}}\omega_i f(t_i)$ □

5. Simulation and performance analysis

5.1. Theoretical validation

To validate the accuracy of analytical approach for both regular path loss model (sparse network) and SPLM (UDN), Monte Carlo simulation is utilized. It is assumed that there is only one user group in these networks. For regular networks with whose BSs are usually located with a low number of density, λ is set at 0.25 BS/km^2 and the path loss exponent is 3.5. In the case of UDNs, the density of BSs λ is selected at 300 BS/km^2 and the tunable parameters are $\beta = 2/3, \alpha = 0.3$. It is seen from Fig. 2, the analytical curves visually match with the corresponding simulation ones. This validates the accuracy of our analytical approach.

5.2. User performance of each group

The tunable parameter of SPLM are selected as $\beta = 2/3$ and $\alpha = 0.3$. The number of users groups is $N = 3$ and four thresholds are adopted as $T_0 = -\infty, T_1 = -15, T_2 = -13, T_3 = \infty$ dB. According to 3GPP recommendations [42], the power ratio
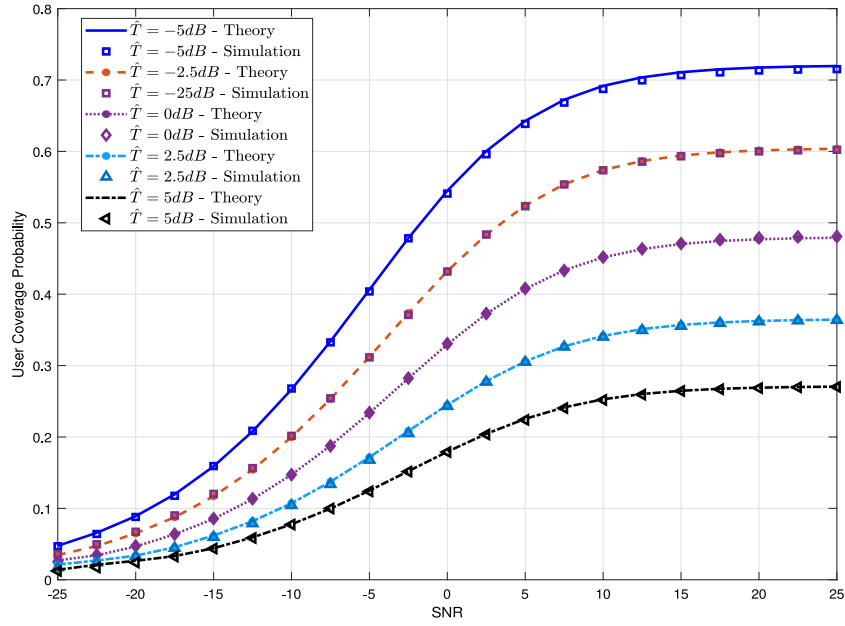
(a) Regular path loss model
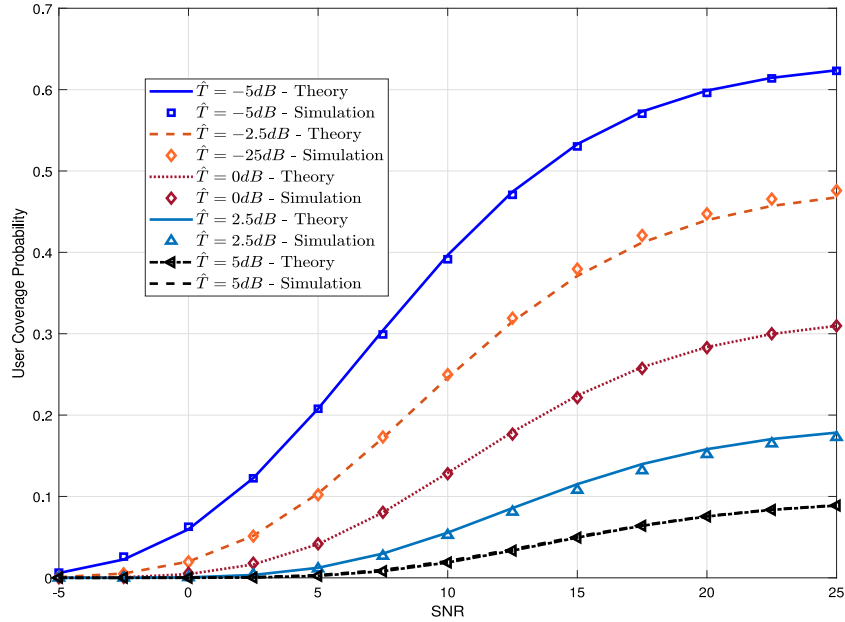
(b) Stretched path loss model

Fig. 2. Simulation and analytical results.

between groups varies from 2 to 20. Thus, the serving powers of user groups are selected as $P_1 = 10P_3, P_2 = 5P_3$. The density of BSs is assumed at $\lambda = 30$ BS/km^2.

With the selection of SINR thresholds, the users in Group 1, 2 and 3 are with downlink SINR on the control channel during the establishment phase in ranges $(-\infty, -15), (-15, -13)$, and $(-13, \infty)$ dB, respectively. However, Fig. 3 indicates that the typical user during the communication phase in Group 1 outperforms others in Group 2 and Group 3. For example, when coverage threshold $\hat{T} = 0$ dB, the coverage probability of the typical user in Group 1 $\mathcal{P}_1 = 0.7112$ which is 1.256 and 1.448 times greater than others in Group 2 and Group 3, respectively. This phenomenon can be explained as follows

- During the communication phase, all users experience the same statistical interference power.
- The serving power of the users in Group 1 is 10 and 5 times greater than those in Group 2 and 3, respectively.

Therefore, the users in Group 1 can experience higher SINRs and consequently better coverage probability.

5.3. Effects of SNR and density of BSs

In Fig. 4, we examine the effects of SNR and the density of BSs on the coverage probability of the typical user in which *SNR* is defined as $SNR = P/\sigma^2$. It is assumed that there are two groups of users $N = 2$. The related parameters are adopted as $\beta = 2/3, \alpha = 0.3$, SINR threshold $T = -5$ dB, coverage threshold $\hat{T} = -10$ dB.
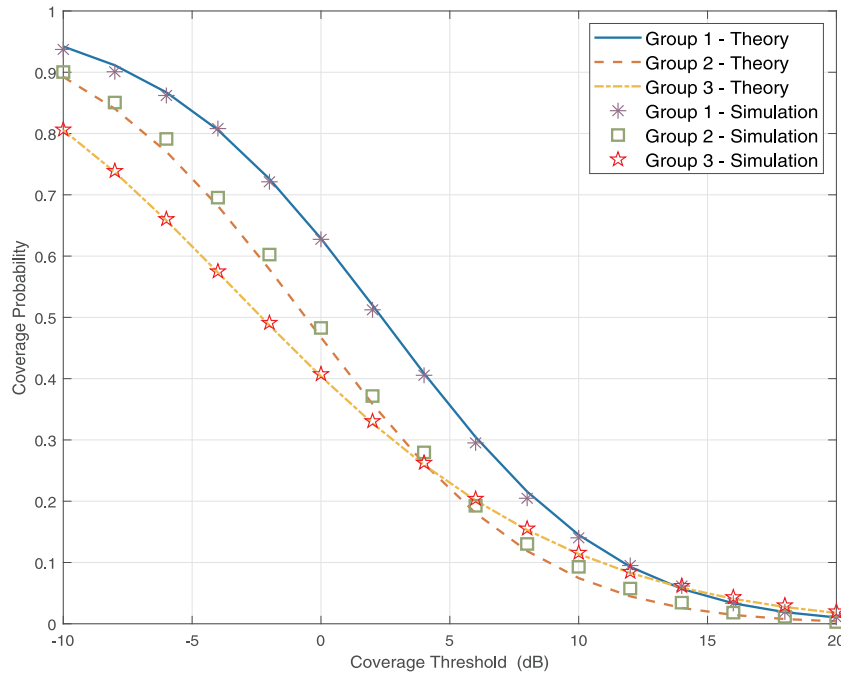
Fig. 3. Coverage probability of user groups.

There are two interesting conclusions that contradicts to other related works on FFR performance analysis in the literature.

(1) Conclusion 1 as shown in Fig. 4a: when the density of BSs λ increases, the user coverage probability increases to the peak if λ is a small regime. Otherwise, it experiences a decline.

(2) Conclusion 2 as shown in Fig. 4b: In high regimes of SNR and λ, increasing the serving power of a user may result in the decline of its performance.

Regarding to Conclusion 1, the authors in [16] stated that the user coverage probability exponentially reduces when λ increases. In addition, the authors assumed that $SNR \approx +\infty$. Hence, the effect of SNR on the network performance was not considered.

In the case of SNR is limited, the downlink SINR from Eqs. (11) and (13) is re-written as follows

$$SINR_n(r) = \frac{gL_r}{I/P_n + 1/SNR} \tag{30}$$

When λ is a small number, i.e. λ in a small regime such as $\lambda < 60$ and $SNR = 20$ dB, an increase in λ leads to the growth of serving power and interfering power which is still small compared to $1/SNR$. Thus, the denominator of Eq. (30) increases at a higher rate than the numerator. Consequently, the received SINR and user coverage probability increase in this case. Specifically, when λ increases from 10 to 40, the user coverage probability rises by 63% from 0.4968 to 0.8905. In contrast, when λ is large enough, an increment in interfering power is obtained when λ increases and be greater than $1/SNR$. Thus, both the received SINR and user coverage probability experience declines.

Regarding Conclusion 2, most of the works in the literature for FFR with two groups of users stated that when transmission power increases, the user performance reaches a peak and keeps constant. However, in a low regime of SNR such as $SNR < 10$ dB and $\lambda = 180$ BS/km², an increase in the transmission power leads to an improvement to the received SINR during the establishment phase [43]. Thus, some users will be pushed from lower groups with high serving powers such as Group 1 to higher groups such as Group 2 with low serving powers. When λ is a small number,

the number of interfering sources and consequently interfering power are relatively smaller than $1/SNR$. Thus, an increase in SNR leads to a significant decline in $1/SNR$ and consequently the interfering power $+ 1/SNR$. Thus, the user coverage probability increases with SNR when λ is relatively small. In contrast, the interfering power is significantly greater than $1/SNR$ if λ is large enough. Therefore, the positive effects of SNR on the user coverage probability reduces with SNR. This may result in a decline in user coverage probability when SNR increases. Take $\lambda = 180$ for example, the user coverage probability is 0.7863 at SNR $= 10$ dB which is 7.6% greater than that at SNR $= 30$ dB. Generally, this conclusion can state that if an increase in the density of BSs is compulsory for UDNs utilizing FFR, then reducing their transmission power is an effective solution.

In the high regime of SNR such as $SNR > 10$ dB and $\lambda = 180$ BS/km², the network is pushed into interference $-$ limited state. Thus, an increase in SNR does not make any remarkable change in SINR during both establishment and communication phases. Hence, the user coverage probability remains unchanged.
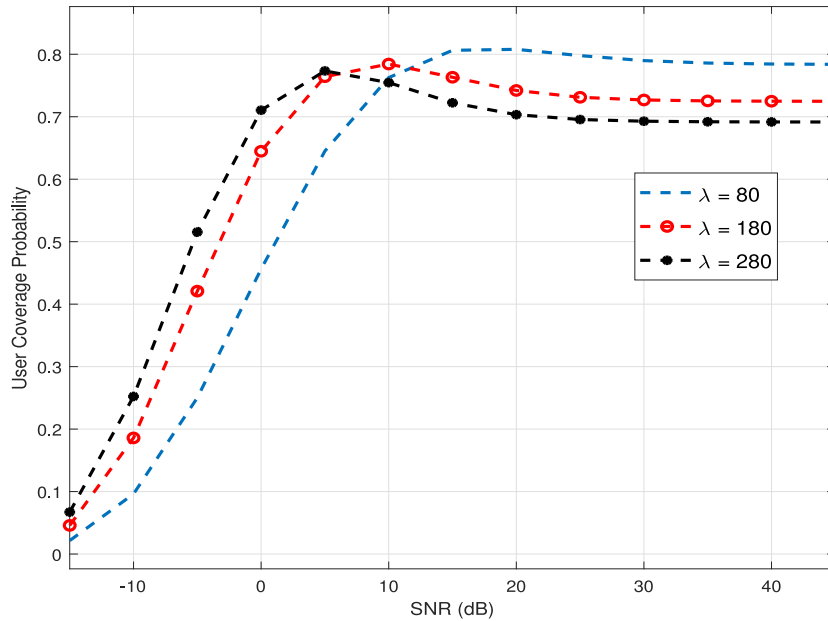
5.4. Effects of the number of user groups

In this section, we compare the user coverage probability for two cases of $N = 2$ and $N = 3$. The transmission power ratios are set at $P_1 : P_2 : P_3 = 10 : 1 : 0.5$ in the case of $N = 3$ and $P_1 : P_2 = 10 : 1$ in the case of $N = 2$. For each value of λ, we find the optimal values of SINR thresholds so that the total power consumption of two cases is the same. Hence, the user coverage probability is computed from Eq. (18). In Fig. 5, the user coverage probability is compared in different channel conditions, particularly different values of α and β.

Since mmWave signal experiences fast attenuation over distances, the received SINR on the downlink of the typical user varies in a large range. Thus, the use of a specific power level may not efficiently improve the performance of users. It is illustrated from Fig. 5 that the system with $N = 3$ outperforms an other with $N = 2$ in all selected channel conditions. Take $\alpha = 3.10^{-1}, \beta = 1$ and the density of BSs is $\lambda = 400$ (BS/km²) for example, the user
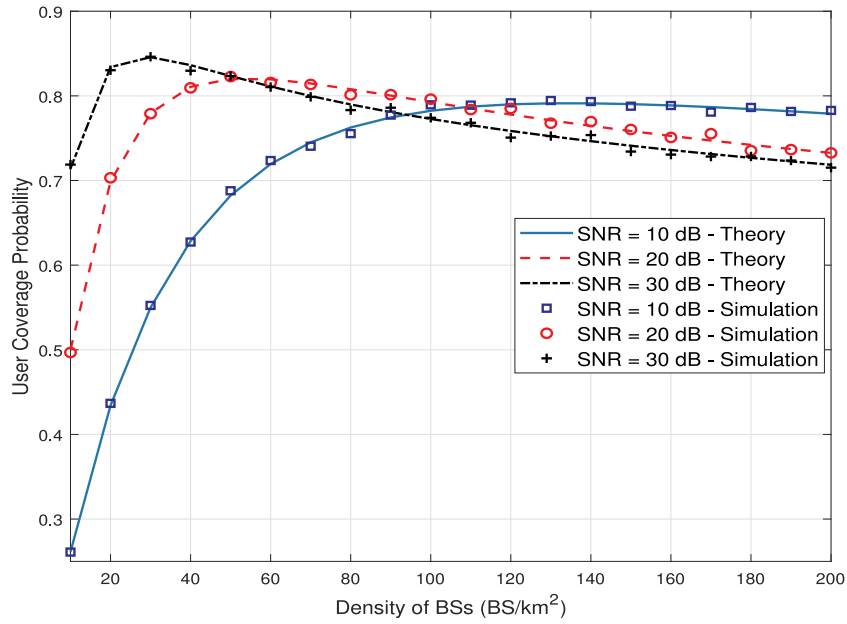
(a) User Coverage Probability vs Density of BSs

(b) User Coverage Probability vs SNR

Fig. 4. Effects of SNR and density of BSs on user performance.

coverage probability increases by 13.55% from 0.541 to 0.6143 when the number of user groups changes from 2 to 3.

The goals of increasing the number of user groups can be explained as follows

- In the case of $N = 2$ with SINR threshold T_1dB, there are some users with very low values of SINR such as $SINR \ll T_1$ dB. These users require a significantly higher power level to achieve acceptable performance. Thus, the serving power $10P$ is a suitable choice for these users. However, there exist users with very high values of $SINR$ such as $SINR \gg T_1$. In other related works in the literature such as [37], it was stated that increasing transmission power cannot improve

the user performance with good received channel conditions. In other words, the users with $SINR \gg T_1$ achieve the same performance when the transmission power is P and lower levels. Since there are only two transmission power levels in the case of $N = 2$, all the users with $SINR > T_1$, including users with $SINR \gg T_1$, are served by transmission power level P. This may result in a waste of power.

- In the case of $N = 3$, three power levels such as $10P$, P and 0.5 are utilized. All the users with $SINR \gg T_1$ are served by the lower power level such as $0.5P$ and they also achieve the similar performance as in the case of serving power P. Meanwhile, compared to the case of $N = 2$, more users with $SINR < T_1$ are served by higher power levels such as $10P$ and $2P$, and achieve significantly higher performance.
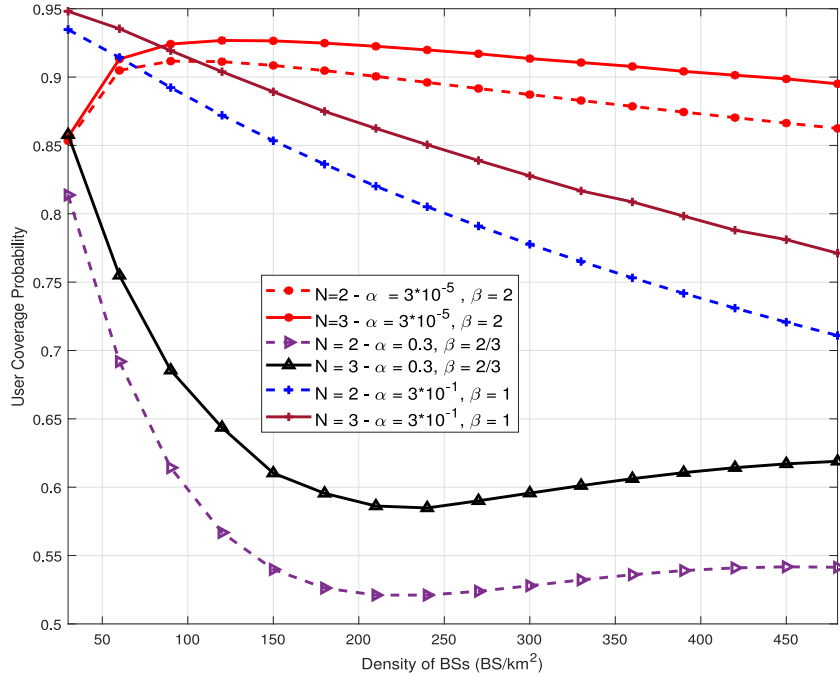
Fig. 5. Effects of number of user groups on user performance.

This results in a significant improvement in user coverage probability as seen in Fig. 5.

6. Conclusion

This paper modeled the UDN network systems utilizing FFR in which the associated users of each BS are classified into N groups. By which each group is served by a predetermined power level. Throughout the mathematical transformation, the user coverage probability was derived. The paper introduced a simple approach to obtain user coverage probability in the case of a general path loss model and the approximated closed-form in the case of SPLM. Through the analytical and simulation results, two interesting statements were found: *(i)* the user coverage probability reaches the peak before passing a decline when the density of BSs increases, *(ii)* an increase in transmission power may result in a decline in user coverage probability. The paper also stated that an increase in the number of user groups can improve the user performance without any additional requirement of BS transmission power, particularly the user coverage probability increases 13.1% when the number of user groups rises from 2 to 3.

Declaration of competing interest

The authors declare that they have no known competing financial interests or personal relationships that could have appeared to influence the work reported in this paper.

Acknowledgment

Appendix A. Proof of Theorem 3.1

The coverage probability of the user at a distance of r from its serving BS which is defined in Eq. (14) can be re-written as follows

$$\mathcal{P}_n^{SINR} = \mathbb{P}\left(SINR_n(r) > \hat{T} \,\middle|\, T_{n-1} < SINR^{(o)}(r) < T_n\right)$$

$$= \frac{\mathbb{P}\left(SINR_n(r) > \hat{T}, T_{n-1} < SINR^{(o)}(r) < T_n\right)}{\mathbb{P}\left(T_{n-1} < SINR^{(o)}(r) < T_n\right)} \tag{A.1}$$

The numerator of Eq. (A.1) is computed as the following steps

$$\mathbb{P}\left(SINR_n(r) > \hat{T}, T_{n-1} < SINR^{(o)}(r) < T_n\right)$$

$$= \mathbb{P}\left(\frac{P_n g L(r)}{I + \sigma^2} > \hat{T}, T_{n-1} < \frac{g^{(o)} L(r)}{I_o + 1/\gamma} < T_n\right)$$

$$= \mathbb{P}\left(g > \hat{T}\frac{I + \sigma^2}{P_n g L(r)}, \frac{T_{n-1}\left(I_o + \sigma^2\right)}{P_N L(r)} < g^{(o)} < \frac{T_n\left(I_o + \sigma^2\right)}{P_N L(r)}\right) \tag{A.2}$$

in which I_o and I are defined in Eqs. (6) and (12). Since g and $g^{(o)}$ are exponential random variables with CDF $f(x) = \exp(-x)$, the probability above can be re-written as follows

$$\mathbb{E}\left[\hat{s}\prod_{k=1}^{N}\prod_{j\in\theta_k}\exp\left(-\hat{T}\frac{P_k g_j L(r_j)}{P_n L(r)}\right)\left(\begin{array}{c} s_{n-1}\prod_{j\in\theta}\exp\left(-\frac{T_{n-1}g_j^{(o)}L(r_j)}{L(r)}\right) \\ -s_n\prod_{j\in\theta}\exp\left(-\frac{T_n g_j^{(o)}L(r_j)}{L(r)}\right) \end{array}\right)\right] \tag{A.3}$$

in which $\hat{s} = \exp\left(-\frac{1}{L(r)}\frac{\hat{T}}{\gamma_n}\right)$ and $s_n = \exp\left(-\frac{1}{L(r)}\frac{T_n}{\gamma_N}\right)$

Taking the expectation with respect to r whose PDF is given by Eq. (1)

$$2\pi\lambda\int_0^\infty \mathbb{E}\left[\begin{array}{c} \hat{s}\prod_{k=1}^N\prod_{j\in\theta_k}\exp\left(-\hat{T}\frac{P_k L(r_j)}{P_n L(r)}g_j\right) \\ \times\left(\begin{array}{c} s_n\prod_{j\in\theta}\exp\left(-T_n\frac{L(r_j)}{L(r)}g_j^{(o)}\right) \\ -s_{n-1}\prod_{j\in\theta}\exp\left(-T_{n-1}\frac{L(r_j)}{L(r)}g_j^{(o)}\right) \end{array}\right) \end{array}\right] \\ \times \exp\left(-\pi\lambda r^2\right)dr \tag{A.4}$$

The expectation in Eq. (A.4) can be expressed as the difference of two expectations in which the second one, denoted by $\zeta(T_n, \hat{T}, r)$ can be evaluated as follows

$$\zeta(T_n, \hat{T}, r)$$

$$= \mathbb{E}\left[\hat{s}s_n \prod_{k=1}^{N}\prod_{j\in\theta_k} \frac{1}{1+\hat{T}\frac{P_k L_{r_j}}{P_n L_r}} \prod_{j\in\theta} \frac{1}{1+\frac{T_{n-1}L_{r_j}}{L_r}}\right]$$

$$= \hat{s}s_n \prod_{k=1}^{N} \mathbb{E}_{\theta_k}\left[\prod_{j\in\theta_k} \frac{1}{1+\hat{T}\frac{P_k L_{r_j}}{P_n L_r}} \frac{1}{1+\frac{T_n L_{r_j}}{L_r}}\right]$$

$$= \hat{s}s_n \prod_{k=1}^{N} \exp\left[-2\pi\lambda_k \int_r^{\infty}\left(1 - \frac{1}{1+\hat{T}\frac{\gamma_k L_{r_j}}{\gamma_n L_r}}\frac{1}{1+T_n\frac{L_{r_j}}{L_r}}\right)r_j dr_j\right]$$

$$= \hat{s}s_n \prod_{k=1}^{N} \exp\left[-\frac{2\pi\lambda_k}{\hat{T}\frac{(\gamma_k)}{\gamma_n}-T_n}\int_r^{\infty}\left[\hat{T}\frac{\gamma_k L_{r_j}}{\gamma_n L_r}\frac{1}{1+\hat{T}\frac{\gamma_k L_{r_j}}{\gamma_n L_r}}\right.\right.$$

$$\left.\left. - T_n^2 \frac{L_{r_j}}{L_r}\frac{1}{1+T_n\frac{L_{r_j}}{L_r}}\right]r_j dr_j\right] \tag{A.5}$$

in which Eq. (A.5) is obtained by assuming that $\hat{T}\frac{\gamma_k L_{r_j}}{\gamma_n L_r} \neq T_n$

As stated in Eq. (13), $r_j \gtrsim r$ is examined in this work. Thus, it can be assumed $\frac{\gamma_k L_{r_j}}{\gamma_n L_r} \approx 1$, $L_{r_j}/L_1 \approx 1$. Hence, these integrals in Eq. (A.5) can be simplified using Taylor series that states [44]

$$\frac{1}{x+1} = \begin{cases} \sum_{m=1}^{M}(-1)^{m-1}x^{-m} & \text{for } x > 1 \\ \sum_{m=0}^{M}(-1)^m x^m & \text{for } x \leq 1, \end{cases} \tag{A.6}$$

Thus the second integral, denoted by $\upsilon(T_n)$, can be expanded as follows

- If $T_n > 1$,

$$\upsilon(T_n) = L_r^{m-1}T_n^{2-m}\sum_{m=1}^{M}(-1)^{m-1}\int_r^{L_{\frac{Lr}{x}}^{-1}} r_j L_{r_j}^{1-m}dr_j$$

$$+ T_n^{m+2}L_r^{-1-m}\sum_{m=0}^{M}(-1)^m\int_{L_{\frac{Lr}{\hat{T}}}^{-1}}^{\infty} r_j L_{r_j}^m dr_j$$

- If $T_n < 1$,

$$\upsilon(T_n) = T_n^{m+2}L_r^{-1-m}\sum_{m=0}^{M}(-1)^m\int_r^{\infty} L_{r_j}^{m+1}r_j dr_j \tag{A.7}$$

Similarly, the first integral in Eq. (A.5) can be expressed as $\upsilon\left(\hat{T}\frac{\gamma_k}{\gamma_n}\right)$. Hence $\zeta(T_n, \hat{T}, r)$ can be re-written as follows

$$\zeta(T_n, \hat{T}, r) = \hat{s}s_n \prod_{k=1}^{N} \exp\left[-\frac{2\pi\lambda_k}{\hat{T}\frac{\gamma_k}{\gamma_n}-T_n}\left(\upsilon\left(\hat{T}\frac{\gamma_k}{\gamma_n}\right) - \upsilon(T_n)\right)\right] \tag{A.8}$$

Similarity, the first expectation in Eq. (A.4) is $\zeta(T_{n-1}, \hat{T}, r)$ which is obtained by replacing $\hat{T}$ in Eq. (A.8) by $\hat{T}\frac{\gamma_k}{\gamma_n}$.

The numerator can be obtained by utilizing above approach for $\hat{T} = 0$. Hence, the numerator is given by

$$2\pi\lambda\int_0^{\infty}\left[s_{n-1}\exp\left[-2\pi\lambda\frac{\upsilon(T_{n-1})}{T_{n-1}}\right] - s_n\exp\left[-2\pi\lambda\frac{\upsilon(T_n)}{T_n}\right]\right]$$

$$\times f(r)dr \tag{A.9}$$

Substituting these results of Eqs. (A.8) into (A.4), and then (A.9) into (A.1), the coverage probability $\mathcal{P}_n$ as in Eq. (15). The Theorem 3.1 has been proved.

Appendix B

Substituting $L_{r_j} = \exp\left(\alpha r_j^\beta\right)$, there integrals of $\upsilon(x)$ can be computed as follows

(1) The first integral

$$\int_r^{L_{\frac{Lr}{x}}^{-1}} r_j L_{r_j}^{1-m}dr_j$$

$$= \int_r^{\left(r^\beta + \frac{\log(x)}{\alpha}\right)^{1/\beta}} r_j \exp\left(-\alpha(1-m)r_j^\beta\right)dr_j$$

$$= \frac{1}{\beta}\int_0^{r^\beta+\frac{\log(x)}{\alpha}} u^{2/\beta-1}\exp\left(-\alpha(1-m)u\right)du$$

$$- \frac{1}{\beta}\int_0^{r^\beta} u^{2/\beta-1}\exp\left(-\alpha(1-m)u\right)du \tag{B.1}$$

$$= \frac{1}{2\alpha^{2/\beta}}\tau_x^{2/\beta}{}_1F_1\left(\frac{2}{\beta}, 1+\frac{2}{\beta}, (m-1)\tau_x\right)$$

$$- \frac{r^2}{2}{}_1F_1\left(\frac{2}{\beta}, 1+\frac{2}{\beta}, (m-1)\tau_1\right) \tag{B.2}$$

in which Eq. (B.1) follows transformation of variable $u = r_j^\beta$, Eq. (B.2) follows [45, p. 348]
Using the properties of confluent hypergeometric function of the first kind, ${}_1F_1(a, b, z) = e^z {}_1F_1(b - a, b, -z)$, then $\int_r^{L_{\frac{Lr}{x}}^{-1}} r_j L_{r_j}^{1-m}dr_j$ equals

$$\int_r^{L_{\frac{Lr}{x}}^{-1}} r_j L_{r_j}^{1-m}dr_j$$

$$= \frac{1}{2\alpha^{2/\beta}}\tau_x^{2/\beta}\exp\left((m-1)\tau_x\right){}_1F_1\left(1, 1+\frac{2}{\beta}, (1-m)\tau_x\right)$$

$$- \frac{1}{2\alpha^{2/\beta}}\tau_1^{2/\beta}\exp\left((m-1)\tau_1\right){}_1F_1$$

$$\times\left(1, 1+\frac{2}{\beta}, (1-m)\tau_1\right) \tag{B.3}$$

- When $2/\beta$ is an integer, the confluent hypergeometric function of the first kind ${}_1F_1$ is obtained by [44, p. 324]

$$_1F_1\left(1, 1+\frac{2}{\beta}, (1-m)\tau_1\right) = \sum_{\omega=1}^{2/\beta}\frac{1}{(2/\beta)!}\left((1-m)\tau_1\right)^{-\omega} \tag{B.4}$$

(2) The second integral $\int_{L_{\frac{Lr}{x}}^{-1}}^{\infty} r_j L_{r_j}^{m+1}dr_j$ is computed as

$$\int_{\left(r^\beta+\frac{\log(x)}{\alpha}\right)^{1/\beta}}^{\infty} r_j \exp(-\alpha(m+1)r_j^\beta)dr_j$$

$$= \frac{1}{\beta}\int_{r^\beta+\frac{\log(x)}{\alpha}}^{\infty} u^{2/\beta-1}\exp(-\alpha(m+1)u)du$$

$$= \frac{1}{\beta}(\alpha(m+1))^{-2/\beta}\Gamma\left(\frac{2}{\beta}, (m+1)\tau_x\right) \tag{B.5}$$

$$= \frac{1}{\beta}(\alpha(m+1))^{-2/\beta}\exp\left(-(m+1)\tau_x\right)$$

$$\times U\left(1-\frac{2}{\beta}, 1-\frac{2}{\beta}, (m+1)\tau_x\right) \tag{B.6}$$

where Eq. (B.5) is obtained by following [45, p. 346] and $\Gamma(x, y)$ is the upper incomplete gamma function; Eq. (B.6) follows the relationship between the incomplete gamma

function and the confluent hypergeometric function of the second kind U [44].

- When $2/\beta$ is an integer, the incomplete gamma function can be computed as $\Gamma(n+1, z) = n! e^{-z} \sum_{k=1}^{n+1} \frac{z^{k-1}}{(k-1)!}$. Hence, the integral becomes

$$\frac{\beta (2/\beta - 1)! x^{-(m+1)}}{(\alpha(m+1))^{2/\beta}} \exp\left(-(m+1)\alpha r^\beta\right) \sum_{u=1}^{2/\beta} \frac{(m+1)^{u-1}\tau_x^u}{(u-1)!}$$

(B.7)

in which Eq. (B.7) follows the binomial expansion. Substituting Eqs. (B.3) and (B.6) into Eq. (9) and changing the sum index from $(0, M)$ to $(1, M+1)$, we get the first case ($x > 0$) of Eq. (25). The result for $x > 0$ in Eq. (26) is obtained by substituting Eqs. (B.3) and (B.7) into Eq. (9).

(3) The third integral for $x < 0$ can be computed in the same manner for the second one, i.e. by letting $x = 1$.

References

[1] Cisco, Cisco visual networking index: Global mobile data traffic forecast update, 2015 ? 2020, 2016.

[2] M. Agiwal, A. Roy, N. Saxena, Next generation 5G wireless networks: A comprehensive survey, IEEE Commun. Surv. Tutor. 18 (3) (2016) 1617–1655.

[3] J.G. Andrews, S. Buzzi, W. Choi, S.V. Hanly, A. Lozano, A.C.K. Soong, J.C. Zhang, What will 5G be? IEEE J. Sel. Areas Commun. 32 (6) (2014) 1065–1082.

[4] W. Yu, H. Xu, H. Zhang, D. Griffith, N. Golmie, Ultra-dense networks: Survey of state of the art and future directions, in: 2016 25th International Conference on Computer Communication and Networks (ICCCN), 2016, pp. 1–10.

[5] M. Kamel, W. Hamouda, A. Youssef, Ultra-dense networks: A survey, IEEE Commun. Surv. Tutor. 18 (4) (2016) 2522–2545.

[6] Y. Zhong, G. Mao, X. Ge, F.-C. Zheng, Spatio-temporal modeling for massive and sporadic access, IEEE J. Sel. Areas Commun. 39 (3) (2021) 638–651.

[7] C. Galiotto, N.K. Pratas, L. Doyle, N. Marchetti, Effect of LOS/NLOS propagation on 5G ultra-dense networks, Comput. Netw. 120 (2017) 126–140, [Online]. Available: http://www.sciencedirect.com/science/article/pii/S1389128617301536.

[8] M. Ding, P. Wang, D. Lopez-Perez, G. Mao, Z. Lin, Performance impact of LoS and NLoS transmissions in dense cellular networks, IEEE Trans. Wireless Commun. 15 (3) (2016) 2365–2380.

[9] I. Atzeni, J. Arnau, M. Kountouris, Downlink cellular network analysis with LOS/NLOS propagation and elevated base stations, IEEE Trans. Wireless Commun. 17 (1) (2018) 142–156.

[10] K. Cho, J. Lee, C.G. Kang, Low-complexity coverage analysis of downlink cellular network for combined LOS and NLOS propagation, IEEE Commun. Lett. 23 (1) (2019) 160–163.

[11] M. Ding, D. Lopez-Perez, Y. Chen, G. Mao, Z. Lin, A. Zomaya, UDN: A holistic analysis of multi-piece path loss, antenna heights, finite users and BS idle modes, IEEE Trans. Mob. Comput. (2019) 1.

[12] M. Ding, D. Lopez Perez, Please lower small cell antenna heights in 5G, in: 2016 IEEE Global Communications Conference (GLOBECOM), 2016, pp. 1–6.

[13] H. Cho, C. Liu, J. Lee, T. Noh, T.Q.S. Quek, Impact of elevated base stations on the ultra-dense networks, IEEE Commun. Lett. 22 (6) (2018) 1268–1271.

[14] M. Franceschetti, J. Bruck, L.J. Schulman, A random walk model of wave propagation, IEEE Trans. Antennas and Propagation 52 (5) (2004) 1304–1317.

[15] D. Ramasamy, R. Ganti, U. Madhow, On the capacity of picocellular networks, in: 2013 IEEE International Symposium on Information Theory, 2013, pp. 241–245.

[16] A. AlAmmouri, J.G. Andrews, F. Baccelli, SINR and throughput of dense cellular networks with stretched exponential path loss, IEEE Trans. Wireless Commun. 17 (2) (2018) 1147–1160.

[17] ETSI TR 102 300-6 V1.1.2, Terrestrial Trunked Radio (TETRA); Voice plus Data (V+D); Designers' guide; Part 6: Air-ground-air, 2016.

[18] A.S. Hamza, S.S. Khalifa, H.S. Hamza, K. Elsayed, A survey on inter-cell interference coordination techniques in OFDMA-based cellular networks, IEEE Commun. Surv. Tutor. 15 (4) (2013) 1642–1670.

[19] Huawei, R1-050507 : Soft frequency reuse scheme for UTRAN LTE, in: 3GPP TSG RAN WG1 Meeting #41, 2005.

[20] L. Yang, W. Zhang, Interference Coordination for 5G Cellular Networks, Springer International Publishing, 2015.

[21] B. Soret, A.D. Domenico, S. Bazzi, N.H. Mahmood, K.I. Pedersen, Interference coordination for 5G new radio, IEEE Wirel. Commun. 25 (3) (2018) 131–137.

[22] B. Singh, O. Tirkkonen, Z. Li, M.A. Uusitalo, Interference coordination in ultra-reliable and low latency communication networks, in: 2018 European Conference on Networks and Communications (EuCNC), 2018, pp. 1–255.

[23] L. Su, C. Yang, C. I, Energy and spectral efficient frequency reuse of ultra dense networks, IEEE Trans. Wireless Commun. 15 (8) (2016) 5384–5398.

[24] N. Al-Falahy, O.Y.K. Alani, Network capacity optimisation in millimetre wave band using fractional frequency reuse, IEEE Access 6 (2018) 10924–10932.

[25] C. Zheng, L. Liu, H. Zhang, Cross-tier cooperation load-adapting interference management in ultra-dense networks, IET Commun. 13 (14) (2019) 2069–2077.

[26] J. Liu, M. Sheng, L. Liu, J. Li, Interference management in ultra-dense networks: Challenges and approaches, IEEE Netw. 31 (6) (2017) 70–77.

[27] T.D. Novlan, R.K. Ganti, A. Ghosh, J.G. Andrews, Analytical evaluation of fractional frequency reuse for OFDMA cellular networks, IEEE Trans. Wirel. Commun. 10 (2011) 4294–4305.

[28] S.C. Lam, K. Sandrasegaran, Performance analysis of fractional frequency reuse in uplink random cellular networks, Phys. Commun. 25 (P2) (2017) 469–482, [Online]. Available: https://doi.org/10.1016/j.phycom.2017.09.008.

[29] X. Liu, Closed-form coverage probability in cellular networks with Poisson point process, IEEE Trans. Veh. Technol. 68 (8) (2019) 8206–8209.

[30] A.I. Aravanis, T.T. Lam, O. Muñoz, A. Pascual-Iserte, M.D. Renzo, A tractable closed form approximation of the ergodic rate in Poisson cellular networks, EURASIP J. Wireless Commun. Networking (2019).

[31] M. Kamel, W. Hamouda, A. Youssef, Uplink coverage and capacity analysis of mMTC in ultra-dense networks, IEEE Trans. Veh. Technol. 69 (1) (2020) 746–759.

[32] L. Cong, N. Tuan, K. Sandrasegaran, A general model of fractional frequency reuse: Modelling and performance analysis, VNU J. Sci.: Comput. Sci. Commun. Eng. 36 (1) (2020).

[33] 3GPP TS 36.101 version 14.3.0 Release 14, LTE; Evolved Universal Terrestrial Radio Access (E-UTRA); User Equipment (UE) radio transmission and reception, 2017.

[34] 3GPP TS 38.101-2 version 15.3.0 Release 15, 5G; NR; User Equipment (UE) radio transmission and reception; Part 2: Range 2 Standalone, 2018.

[35] 3GPP TS 36.213 version 8.8.0 Release 8, LTE; Evolved Universal Terrestrial Radio Access (E-UTRA); Physical layer procedures, 2009.

[36] ETSI TS 136 423 V15.5.0, LTE; Evolved Universal Terrestrial Radio Access Network (E-UTRAN); X2 Application Protocol (X2AP) , 2019.

[37] J.G. Andrews, F. Baccelli, R.K. Ganti, A tractable approach to coverage and rate in cellular networks, IEEE Trans. Commun. 59 (11) (2011) 3122–3134.

[38] S. Zhang, Inter-Cell Interference Coordination in Indoor LTE Systems (Masters Thesis), 2011.

[39] GSMA, 4G/5G network experience evaluationguideline, 2020.

[40] J.G. Andrews, F. Baccelli, R.K. Ganti, A new tractable model for cellular coverage, in: 2010 48th Annu. Allerton Conference on Communication, Control, and Computing (Allerton), pp. 1204–1211.

[41] M.A. Stegun, I. A., Handbook of Mathematical Functions with Formulas, Graphs, and Mathematical Tables, ninth ed., Dover Publications, 1972.

[42] 3GPP TR 36.828 V11.0, E-UTRA further enhancements to LTE time division duplex (TDD) for downlink-uplink (DL-UL) interference management and traffic adaptation, 2012.

[43] S.C. Lam, H. Danh Huynh, Q.T. Nguyen, K. Sandrasegaran, Strict frequency reuse in ultra dense networks, in: TENCON 2018 - 2018 IEEE Region 10 Conference, 2018, pp. 1027–1032.

[44] F. Olver, D. Lozier, R. Boisvert, C. Clark, NIST Handbook of Mathematical Functions, 2010.

[45] A. Jeffrey, D. Zwillinger, I. Gradshteyn, I. Ryzhik (Eds.), 3 - 4 - Definite integrals of elementary functions, in: Table of Integrals, Series, and Products (Seventh Edition), seventh ed., Academic Press, Boston, 2007, pp. 247–617, [Online]. Available: http://www.sciencedirect.com/science/article/pii/B9780080471112500133.

Sinh Cong Lam received the Bachelor of Electronics and Telecommunication (Honours) and Master of Electronic Engineering in 2010 and 2012, respectively from University of Engineering and Technology, Vietnam National University (UET, VNUH). He obtained his Ph.D. degree from University of Technology, Sydney, Australia. His research interests focus on modeling, performance analysis and optimization for 4G and 5G, stochastic geometry model for wireless communications

Xuan Nam Tran received his master of engineering (M.E.) in telecommunications engineering from University of Technology Sydney, Australia in 1998, and doctor of engineering in electronic engineering from The University of Electro-Communications, Japan in 2003. From November 2003 to March 2006 he was a research associate at the Information and Communication Systems Group, Department of Information and Communication Engineering, The University of Electro-Communications, Tokyo, Japan . Since April 2006 he has been with Le Quy Don Technical University. Professor Xuan Nam Tran is currently Head of Strong Research Group on Advanced Wireless Communications and Head of Office of Academic Affairs, Le Quy Don Technical University, Vietnam.